ISSN 2518–2021 (Print) 2415–4474 (Electronic)

Fundamental and Applied Agriculture

Journal home page: https://www.f2ffoundation.org/faa/index.php/home

Vol. 10(1), pp. 333 – 349: 2025, doi: https://doi.org/10.5455/faa.265943

AGRICULTURE | ORIGINAL ARTICLE

# Green-Synthesized Ag and ZnO Nanoparticles using *Cassia fistula* Leaf Extract: Biocompatibility and Growth Response in Early Plant Development

**A H M Maniruzzaman Rabbani[1,2], Syeda Nyema Jannat[1], Md Shahed Al Shishir[1], Md Shaheen Alam[1], Atiqur Rahman[1], Md Shohidul Alam[1] ✉**

[1] Department of Agricultural Chemistry, Bangladesh Agricultural University, Mymensingh 2202, Bangladesh

[2] Department of Agricultural Extension, Ministry of Agriculture, Khamarbari, Dhaka 1207, Bangladesh

**ARTICLE INFO**

**Article history**

Received: 13 Feb 2025

Accepted: 21 Mar 2025

Published online: 31 Mar 2025

**Keywords**

Green synthesis, *Cassia fistula,* Silver nanoparticles, Zinc oxide nanoparticles, Seed germination, Early plant development

**Correspondence**

Md Shohidul Alam

✉: shohidul.alam@bau.edu.bd

**ABSTRACT**

Green synthesis of metal nanoparticles offers an eco-friendly alternative to conventional chemical methods, with promising applications in agriculture. However, the phytotoxicity of such nanoparticles (NPs), particularly silver (Ag-NPs) and zinc oxide (ZnO-NPs), remains poorly understood. This study investigates the green synthesis, characterization, and biological effects of Ag-NPs and ZnO-NPs using aqueous leaf extracts of *Cassia fistula*, a plant rich in phytochemicals. UV-Vis spectroscopy confirmed successful synthesis, revealing characteristic peaks at 479 nm (Ag-NPs) and 241 nm (ZnO-NPs). Energy band gaps were calculated as 2.34 eV for Ag-NPs and 4.13 eV for ZnO-NPs. To assess biocompatibility and phytotoxicity, the nanoparticles were tested on seed germination, root and shoot growth, and biomass accumulation in five crop species: *Oryza sativa* (rice), *Brassica napus* (canola), *Raphanus sativus* (radish), *Solanum lycopersicum* (tomato), and *Ipomoea aquatica* (water spinach). Both NPs showed concentration-dependent effects: low to moderate doses enhanced germination and seedling vigor, whereas higher doses delayed germination and reduced growth. Ag-NPs were generally more phytotoxic, particularly inhibiting root elongation. ZnO-NPs exhibited a biphasic response - stimulatory at lower concentrations, inhibitory at higher levels. Seedling biomass decreased with increasing NP concentration, with Ag-NPs causing more severe reductions.These findings highlight that while green-synthesized nanoparticles hold agricultural potential, their use must be carefully optimized to avoid phytotoxic effects. The *Cassia fistula*-mediated synthesis presents a sustainable, biocompatible route for generating functional nanoparticles capable of influencing early plant development.



## 1. Introduction

Nanotechnology has rapidly gained traction in agriculture due to its potential to enhance crop productivity, disease resistance, and nutrient delivery (Chand Mali *et al.*, 2020; Rana *et al.*, 2024; Zaman *et al.*, 2025). Among the most widely studied nanomaterials are silver (Ag) and zinc oxide (ZnO) nanoparticles, which are known for their antimicrobial, antioxidant, and growth-modulating properties (Jobe *et al.*, 2022; Mohamed *et al.*, 2024). However, their unintended phytotoxic effects raise concerns about their safe integration into agricultural systems (Madanayake and Adassooriya, 2021; Muzammil *et al.*, 2023).Conventional methods for synthesizing nanoparticles often involve toxic chemicals and energy-intensive processes (Osman *et al.*, 2024; Vishwanath and Negi, 2021). In contrast, green synthesis utilizes plant extracts, offering a cost-effective and environmentally benign alternative(Saxena *et al.*, 2025). These biogenic nanoparticles are thought to be more compatible with living systems(Maqsood *et al.*, 2023), yet their interactions with plant tissues during critical growth stages such as germination remain insufficiently explored.

Seed germination and early seedling development are highly sensitive to environmental stresses, including nanoparticle exposure (Bayat *et al.*, 2022; Rutkowski *et al.*, 2024; Szőllősi *et al.*, 2020). The degree of phytotoxicity can vary depending on the nanoparticle type, concentration, and the crop species involved (Sembada and Lenggoro, 2024). Previous studies suggest that Ag-NPs tend to be more phytotoxic than ZnO-NPs due to their

**Cite This Article**

Rabbani AHMM, Jannat SN, Al Shishir MS, Alam MS. Rahman A, Alam MS. 2025. Green-Synthesized Ag and ZnO Nanoparticles using *Cassia fistula* Leaf Extract: Biocompatibility and Growth Response in Early Plant Development. *Fundamental and Applied Agriculture*, 10(1): 333–349. https://doi.org/10.5455/faa.265943

higher reactivity and potential to disrupt cellular processes (Malandrakis *et al.*, 2021).

This study aims to assess the comparative biocompatibility and growth response of green-synthesized Ag and ZnO nanoparticles on five economically important crops: rice, canola, radish, tomato, and water spinach. Specifically, the effects on seed germination, shoot and root length, and seedling biomass were evaluated under controlled conditions.

## 2. Materials and Methods

### 2.1. Experimental site

The experiment was conducted at the post-graduate laboratories and Materials for Sustainable Agriculture (MSA) Laboratory of the Department of Agricultural Chemistry, Bangladesh Agricultural University, Mymensingh-2202. The seed germination tests were performed in the laboratory of the Department of Agricultural Chemistry, Bangladesh Agricultural University.

### 2.2. Plants selected for green synthesis of metal nanoparticles

For this study, native plants known for their use in the green synthesis of metal nanoparticles were surveyed, and Sonalu (*Cassia fistula*) was selected due to its local availability and rich phytochemical profile. The plant belongs to the Fabaceae family and is a deciduous tree growing 15 to 20 meters tall, thriving in medium to high altitude areas. It sheds its leaves in winter and produces new leaves in late spring before flowering, with golden-yellow flowers blooming throughout summer. The tree has light green leaves with a prominent midvein, few straight upward-growing branches, greenish-gray bark, and medium-hard wood. Its fruit resembles a vegetable pod, initially green but turning dark brown when ripe, containing seeds used for propagation; locally, the fruit is sometimes called "monkey stick," and the tree is also known as the monkey stick tree. Both bark and leaves of *C. fistula* exhibit medicinal properties including antibacterial, antioxidant, hepatoprotective, and hypoglycemic effects, and have been used to treat ailments like diarrhea and polyuria. Phytochemical screening of Sonalu leaves indicates the presence of bioactive primary and secondary metabolites, particularly polar compounds extractable with water. Due to these properties, several studies have successfully synthesized metallic nanoparticles using aqueous extracts of *C. fistula* leaves, making it a suitable candidate for green nanoparticle synthesis in this research.

### 2.3. Chemicals and reagents

Silver nitrate ($AgNO_3$) Extra pure and zinc acetate dehydrate ($Zn(CH_3COO)_2{\cdot}2H_2O$).Extra pure were purchased from www.researchlab.in. All other chemicals used were of analytical grade and high purity and were procured from reputed firms.

### 2.4. Collection of plant material

Leaves of *C. fistula* were collected from different farm area of Bangladesh Agricultural University campus, Mymensingh.

### 2.5. Preparation of leaf extract

To prepare leaf extract, fresh leaves of selected plants were thoroughly washed with tap water followed by distilled water to remove any contamination or dust or unwanted particles that could interfere with the adhesion of $Ag^+$ and $Zn^{2+}$ ions during the synthesis process. About 200 g of leaves were chopped into small pieces and combined with 500 mL of deionized water. After fine blending in an electric blender, the mixture was heated at 70°C for 30minutes to release intracellular material into the solution. The mixture was then cooled and filtered through Whatman No. 1 filter paper. The resulting filtrate was stored at 4°C before being used in the green synthesis of silver and zinc oxide nanoparticles.

### 2.6. Green synthesis of silver and zinc oxide nanoparticles using *Cassia fistula* leaf extract

Silver and zinc oxide nanoparticles were synthesized via green chemistry approaches' using aqueous leaf extracts of *C. fistula* as natural reducing, capping, and stabilizing agents, following methods adapted from Faisal et al. (2021).

#### *2.6.1. Synthesis of silver nanoparticles (Ag-NPs)*

A 0.1 M solution of extra pure silver nitrate ($AgNO_3$) was prepared using deionized water. For the synthesis of silver nanoparticles, 90 mL of the $AgNO_3$ solution was mixed with 10 mL of *C. fistula* leaf extract in a 250 mL conical flask. The plant extract was added dropwise using a burette under constant stirring (150 rpm) on a magnetic stirrer, and the mixture was incubated at 70 °C for 1 hour. A visible color change from colorless to light yellow and eventually to brown indicated the reduction of $Ag^+$ ions to elemental silver ($Ag^0$), confirming the formation of silver nanoparticles (Fig.1). To prevent photo-activation, the reaction mixture was stored in a dark chamber at room temperature. The synthesized nanoparticles were purified by centrifugation at 4000 rpm for 30 minutes, washed thrice with deionized water to remove residual impurities, and stored at 4 °C for further characterization.

#### *2.6.2. Synthesis of zinc oxide nanoparticles (ZnO-NPs)*

Zinc oxide nanoparticles were synthesized using a similar protocol. A 0.01 M solution of zinc acetate dihydrate [$Zn(CH_3COO)_3{\cdot}2H_2O$] was prepared in deionized water. For each synthesis, 90 mL of the zinc acetate solution was combined with 10 mL of *C. fistula* leaf extract in a 250 mL conical flask.

The plant extract was added dropwise while stirring continuously at 150 rpm and incubated at 70 °C for 1 hour, following the method described by Naseer et al. (2020). A gradual color change from colorless to off-white or light brown, accompanied by the formation of a white precipitate, indicated the bio-reduction of zinc ions and the formation of ZnO nanoparticles (Fig.1). The supernatant was carefully decanted, and the precipitated nanoparticles were transferred into 15 mL centrifuge tubes. The samples were washed three times with deionized water by centrifugation at 4000 rpm for 30 minutes to ensure purity. The purified ZnO-NPs were stored at 4 °C for further analysis.

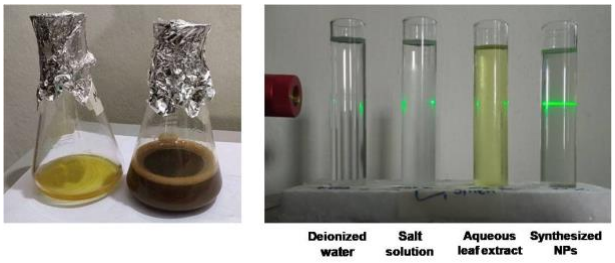


Figure 1. Colour change indicating formation of nanoparticles

### 2.7. Characterization of Ag-NPs and ZnO-NPs by UV-visible spectral analysis and scanning electron microscopy (SEM)

Green synthesized Ag-NPs and ZnO-NPs were characterized by UV-Vis spectroscopy and SEM. UV–vis spectra were recorded to check the reduction of silver nitrate with selected plant leaf extract using a T60 UV-Visible Spectrophotometer (PG Instruments) in the range of 300–600 and 1 nm resolution. UV–vis spectra of the AgNPs peak at 420 nm after 3 h incubation. UV–visible spectroscopy is one of the most widely used techniques for structural characterization of nanoparticles (Hemlata *et al.*, 2020). The presence of an absorbance peak at about 420 nm clearly indicates the formation of Ag-NPs in the solution due to surface plasmon resonance (SPR) electrons present on the nanoparticle surface. The SPR pattern is dependent on the characteristics of the individual metal particles, such as size and shape, as well as the dielectric properties of the medium used for synthesis and the inter-nanoparticle coupling interactions. The intensity of the SPR band increased with reaction time, indicating the synthesis of the AgNPs (Khlebtsov *et al.*, 2005).

The bioreduction of zinc oxide was confirmed by subjecting diluted aliquots of the zinc metallic NPs to T60 UV-Visible Spectrophotometer (PG Instruments) in the range of 150-350 nm and 1 nm resolution (Gupta *et al.*, 2018; Talam *et al.*, 2012). The deionized $H_2O$ was used as a reference. Energy gap or band gap was calculated using the following equation.

$$\mathrm{Eg} = \frac{1239.83}{\lambda nm}$$

Where, Eg is the bulk band expressed in eV. Lambda (λ) is peak absorbance wavelength in nm (Naseer *et al.*, 2020).

The smaller band gap will easily categorize a photocatalytic reaction of the nanoparticles and show good photocatalytic activity for the degradation of methylene blue dye. Because of the smaller band gap, the electron is easily excited from the valence band to the conduction band. The band gap depends on various factors, including the grain size, oxygen deficiency, surface roughness, and lattice strain (Faisal *et al.*, 2021; Wang and Chang, 2016). The synthesized nanoparticles were subjected to Scanning Electron Microscopy (SEM) for further characterization.

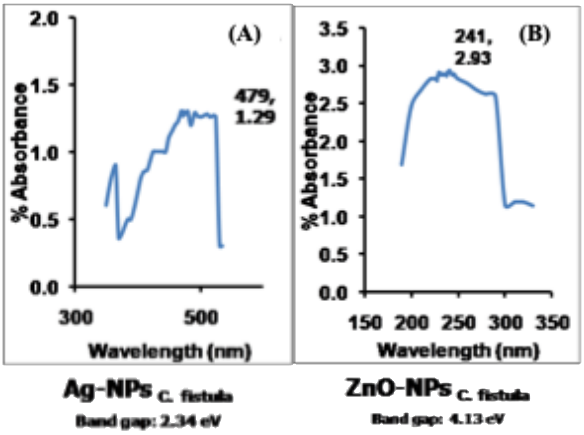


Figure 2. UV-visible absorption spectrum confirming presence of C. fistula mediated Ag-NPs (A) and ZnO-NPs (B)

### 2.8. Seed germination and vegetative growth test

The effects of synthesizedAg-NPs and ZnO-NPs on the seed germination and seedling growth of Rice (*Oryza sativa*) cv. BRRI dhan 29, Canola (*Brassica napus*) cv. BARI Sarisha-18, Radish (*Raphanus sativus*) cv. BARI Mula-1 (Tasakisan), Tomato (*Solanum lycopersicum*) cv. BARI Tomato-2 (Ratan), Water spinach (*Ipomoea aquatica*) cv. Gima kalmi were studied. The vegetative growth parameters including % seed germination, shoot length, root length, fresh weight of seedlings were evaluated (Aslani *et al.*, 2014; Gopinath *et al.*, 2014; Umavathi *et al.*, 2021) Germination tests with nanoparticles solution at different concentrations were done on Petri dishes of 9 cm in diameter with 3-5 layers of tissue papers and under tissue papers a thin layer of sterilized cotton was placed.

For seed germination 10 to 20 healthy seeds of each test crop were placed in each Petri dish on layers of tissue paper. Each treatment was moistened with 20 mL nanoparticles solution of 5 different concentrations (0, 25, 50, 75 and 100 mg $L^{-1}$). For control treatment seeds were moistened with 20 mL deionized water. Three replicates of each treatment were used in these experiments and arranged under a Completely Randomized Design (CRD) and there was total 5 treatments. The Petri dishes were kept on a table at room temperature (~25 °C) under 12 hours light condition provided with white LED lights. Each day, 5 mL deionized water was added in each Petri dish. The number of seeds that had germinated was recorded on 3, 7 and 14 days after seed sowing.

Seeds were considered to have germinated when the emerging radical was at least 2 mm long. The germination test was continued up to 14 days after seed sowing (DAS) and per cent germination was calculated. The shoot length, root length and fresh weight of seedling were taken after completion of the germination test.

### 2.9. Statistical analysis

Data were analyzed in a grouped analysis by ANOVA using GraphPad Prism software followed by Tukey's post hoc test to determine significant differences among treatments at $p < 0.05$.

## 3. Results and Discussion

### 3.1. Characterization of synthesized Ag-NPs and ZnO-NPs

Adding aqueous leaf extract of *C. fistula* in silver nitrate solution, leads to physio-chemical changes in the mixture. The most prominent of which is change in the colour of the reaction mixture that can be observed within few minutes. This was considered as an initial signature to formation of NPs. In present study, change of color from green to light yellow brown indicated the formation of Ag-NPs with leaf extracts of *C. fistula*. Flavonoides and phenolic compounds are thought to be responsible for Ag ions to Ag-NPs (Jain and Mehata, 2017). In a period of few hours, the colour of the solution stopped changing further suggesting the complete bioreduction of Ag salt into NPs. A clear illustration of change in color of the reaction mixtures due to formation of Ag NPs has been shown in Fig. 1(A). These results were consistent with the previous reports of color changes in plant based synthesis of Ag-NPs (Jain and Mehata, 2017; Saware and Venkataraman, 2014). Temperature is considered an important contributing factor in synthesis of good sized nanoparticles. It is also well established that higher the temperature of reaction processes of NPs synthesis, the smaller the size of the NPs (Jain and Mehata, 2017; Saware and Venkataraman, 2014). Therefore, we use a relatively higher temperature of 70 °C for incubating the reactants that leads to the production of very small sized Ag-NPs. The synthesis of Ag-NPs was further examined by UV spectrophotometry. Figure 2 shows the UV peaks recorded by the spectrophotometer. The maximum absorption peak for Ag-NPs synthesized via *C. fistula* was recorded at 479 nm, which further verified the formation of Ag-NPs (Fig. 2A). The energy gap for synthesized Ag-NPs was 2.34 eV which was supported by previous report on Ag-NPs energy gap 2.51 eV (Aziz *et al.*, 2018).

Adding aqueous leaf extract of *C. fistula* in zinc acetate dihydrate solutionleads to physio-chemical changes in the mixture. The most prominent of which is change in the colour of the reaction mixture that can be observed within few minutes. This was considered as an initial signature to formation of NPs. In present study, change of color from green to light yellow brown indicated the formation of ZnO-NPs in leaf extracts of *C. fistula*. Flavonoides and phenolic compounds are thought to be responsible for Zn ions to ZnO-NPs (Jain and Mehata, 2017). In a period of few hours, the colour of the solution stopped changing further suggesting the complete bioreduction of Zn salt into NPs. A clear illustration of change in color of the reaction mixtures due to formation of ZnO-NPs has been shown in Fig.1. These results were consistent with the previous reports of color changes in plant based synthesis of ZnO-NPs (Rajiv *et al.*, 2013). Temperature is considered an important contributing factor in synthesis of good sized nanoparticles. It is also well established that higher the temperature of reaction processes of NPs synthesis, the smaller the size of the NPs (Jain and Mehata, 2017; Saware and Venkataraman, 2014). Therefore, we use a relatively higher temperature of 70 °C for incubating the reactants that leads to the production of very small sized ZnO-NPs. The synthesis of ZnO-NPs was further examined by UV spectrophotometry. Fig.2(B) shows the UV peaks recorded by the spectrophotometer. The maximum absorption peak for ZnO-NPs synthesized via *C. fistula* was recorded at 241 nm that further verified the formation of ZnO-NPs (Fig.2B). Firstly, these results satisfy standard ZnO absorption pattern because all oxide materials have wide band gaps and tend to have shorter wavelengths.

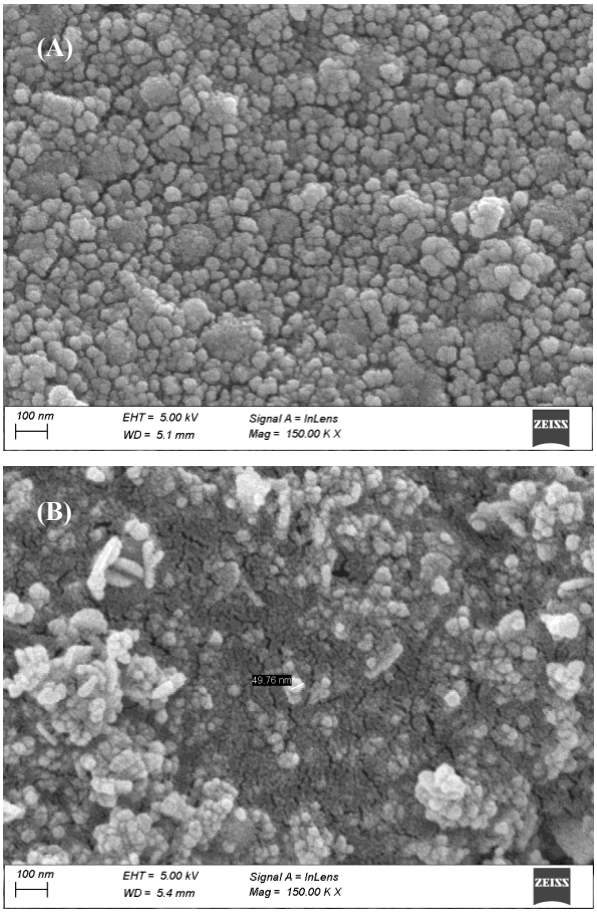


Figure 3. SEM micrographs of green-synthesized (A) silver (Ag-NPs) and (B) zinc oxide (ZnO-NPs) nanoparticles

The energy gap for synthesized ZnO-NPs was found 4.13 which were supported by previous report on ZnO-NPs energy gap for ranged from 4.27–3.87 eV (Brus, 1986; Naseer *et al.*, 2020).

Moreover, if the material is of nanoscale, it tends to have further shorter wavelengths. This notion support the results observed for ZnO-NPs here (Naseer *et al.*, 2020; Zhang *et al.*, 2002). The SEM micrographs of green-synthesized silver (Ag-NPs)(Fig. 3A) and zinc oxide (ZnO-NPs) nanoparticles(Fig. 3B) further characterized the synthesized nanoparticles.

### 3.2. Effect of green synthesized Ag-NPs and ZnO-NPs on seed germination

Seed germination is a critical stage in the life history of individual plants. Effect of different concentration of green synthesized Ag-NPs and ZnO-NPs on germination of seeds and early seedling growth were recorded and analyzed.The effect of *C. fistula*-mediated green-synthesized silver nanoparticles (AgNPs) on seed germination of *Oryza sativa* cv. BRRI dhan29 was evaluated across varying concentrations (0, 25, 50, 75, and 100 mg $L^{-1}$) over a 14-day period. No germination was observed in any treatment at 0 days after sowing (DAS). By 3 DAS, seeds treated with 25 and 50 mg $L^{-1}$ AgNPs exhibited higher germination percentages (50%) than the control (40%), indicating a slight stimulatory effect at lower concentrations. At 7 DAS, the highest germination rate (80%) was recorded at 25 mg $L^{-1}$, closely followed by 50 mg $L^{-1}$ (70%). However, the 75 mg $L^{-1}$ treatment showed a reduced germination rate (60%), suggesting possible inhibitory effects at this intermediate concentration (Fig. 4 A). By 10 DAS, a significant increase was observed in the 100 mg $L^{-1}$ treatment, reaching a germination rate of 100%, the highest among all treatments. In contrast, germination in other treatments plateaued or increased modestly, with the control reaching 86.7%, and the 25 and 50 mg $L^{-1}$treatments achieving 73.3% and 80%, respectively. The 75 mg $L^{-1}$treatment remained relatively low at 70%. This trend persisted through 14 DAS, confirming that the 100 mg $L^{-1}$AgNP treatment significantly enhanced seed germination compared to the control and other concentrations (Fig. 4 A).

These results suggest a concentration-dependent response of rice seeds to AgNP exposure. While lower concentrations (25–50 mg $L^{-1}$) stimulated early germination, they did not result in the highest final germination percentages. In contrast, the highest concentration (100 mg $L^{-1}$) exhibited a delayed yet substantial enhancement in germination, potentially due to increased metabolic activity or bioavailability of nanoparticles over time. The reduced germination at 75 mg $L^{-1}$may reflect a threshold above which AgNPs begin to exhibit phytotoxic effects. These findings highlight the potential of green-synthesized silver nanoparticles to enhance seed germination, particularly at higher concentrations, though proper dosage is essential to avoid negative outcomes. Similarly, the effect of *Cassia fistula*-mediated green-synthesized zinc oxide (ZnO) nanoparticles was assessed at the same concentration range (0, 25, 50, 75, and 100 mg $L^{-1}$). No germination occurred at 0 DAS in any treatment. By 3 DAS, both the control and 25 mg $L^{-1}$ZnO treatments showed the highest early germination rates (40%), while the 50 and 75 mg $L^{-1}$treatments were slightly lower (30%). Notably, no germination was observed at this time in the 100 mg $L^{-1}$treatment, indicating a delayed germination response at high ZnO concentrations (Fig. 4 F). A sharp increase in germination was observed by 7 DAS in the 25 mg $L^{-1}$ treatment, reaching 100%, significantly outperforming all other concentrations. The control and 50 mg $L^{-1}$ treatments reached moderate germination levels (60–70%), while the 75 mg $L^{-1}$and 100 mg $L^{-1}$ treatments lagged behind (60% and 50%, respectively). This highlights a strong promotive effect of 25 mg $L^{-1}$ ZnO on early seed germination (Fig. 4 F).

At both 10 and 14 DAS, the 25 mg $L^{-1}$ZnO treatment maintained 100% germination, while the control, 50 mg $L^{-1}$, 75 mg $L^{-1}$, and 100 mg $L^{-1}$treatments all reached comparable final germination percentages of 80–90%. Although the higher concentrations eventually caught up to the control in terms of final germination, the delay observed, particularly at 100 mg $L^{-1}$, suggests a transient inhibitory effect at higher nanoparticle concentrations. These findings indicate that ZnO nanoparticles also exert a concentration-dependent effect on seed germination. However, unlike AgNPs, ZnO nanoparticles were most effective at a lower concentration (25 mg $L^{-1}$), both in terms of early and final germination performance. Higher concentrations (≥50 mg $L^{-1}$) did not improve final germination and, in some cases, appeared to delay the process—likely due to stress or toxicity effects induced by excessive nanoparticle exposure. In contrast to the AgNP treatment, where the highest concentration (100 mg $L^{-1}$) led to the most significant germination improvement, ZnO nanoparticles showed optimal efficacy at lower doses. Together, these results underscore the importance of optimizing both the type and concentration of nanoparticles used in agricultural applications. While green-synthesized nanoparticles offer promising potential for improving seed germination and early plant growth, their effects are not uniform and require careful evaluation to ensure maximum benefit without adverse outcomes.

The influence of *Cassia fistula*-mediated green-synthesized silver nanoparticles (AgNPs) on seed germination of *Solanum lycopersicum* cv. BARI Tomato-2 was evaluated at concentrations of 0, 25, 50, 75, and 100 mg $L^{-1}$ over a 7-day period. No germination was observed in any treatment at 0 days after sowing (DAS), indicating uniform seed dormancy across treatments. By 3 DAS, a significant variation in germination rates was recorded. Seeds treated with 25 mg $L^{-1}$ AgNPs exhibited the highest germination rate (90%), significantly surpassing the control (70–80%). In contrast, the 50 mg $L^{-1}$treatment showed markedly lower germination (50%), suggesting potential inhibitory effects at this concentration. The 75 mg $L^{-1}$ and 100 mg $L^{-1}$ treatments resulted in moderate germination levels (60% and 70%, respectively) (Fig. 4 b).

By 7 DAS, no further changes in germination were observed, indicating that peak germination had occurred within the first three days. The 25 mg $L^{-1}$AgNP treatment maintained its superior performance (90%), while the control remained at an average of 76.7%. The 50 mg $L^{-1}$ treatment remained the least effective, maintaining its earlier germination percentage (50%). Interestingly, both the 75 and 100 mg $L^{-1}$ treatments plateaued at 70%, suggesting that higher AgNP concentrations were not severely phytotoxic but also did not confer additional germination benefits (Fig. 4B). These results indicate a concentration-dependent effect of AgNPs on tomato seed germination. The 25 mg $L^{-1}$ treatment emerged as the most effective, likely due to an optimal balance between nanoparticle-induced physiological stimulation and

minimal stress. Higher concentrations, especially 50 mg $L^{-1}$, may have caused oxidative or osmotic stress, leading to suppressed germination. The recovery observed at 100 mg $L^{-1}$, albeit not exceeding the control, suggests a potential threshold effect where toxicity may decline or plants adapt metabolically.

In a parallel assessment, *Cassia fistula*-mediated green-synthesized zinc oxide (ZnO) nanoparticles were applied at the same concentrations. As with AgNPs, no germination was recorded at 0 DAS. By 3 DAS, seeds treated with 25 and 50 mg $L^{-1}$ZnO nanoparticles achieved full germination (100%), clearly outperforming all other treatments. The 75 mg $L^{-1}$treatment resulted in a moderate germination rate (80%), while the control and 100 mg $L^{-1}$treatments recorded 76.7% and 70%, respectively (Fig. 4 G). No further changes in germination were recorded at 7 DAS, confirming that the maximum germination potential was reached early. The 25 and 50 mg $L^{-1}$treatments consistently maintained 100% germination, indicating strong and immediate positive effects on seed performance. The 75 and 100 mg $L^{-1}$treatments settled at 80%, with the 100 mg $L^{-1}$treatment showing slight improvement over the initial 3 DAS data. The control remained stable at 76.7%. These findings highlight that ZnO nanoparticles also produce a concentration-dependent germination response. However, unlike AgNPs, the ZnO nanoparticles exhibited no evidence of suppression at 50 mg $L^{-1}$, instead showing optimal enhancement at both 25 and 50 mg $L^{-1}$. The reduced performance at 75 and 100 mg $L^{-1}$may reflect mild nanoparticle-induced stress, though not to the extent observed with AgNPs at comparable concentrations.

Both nanoparticle types demonstrated the potential to improve tomato seed germination, but with differing optimal concentrations. AgNPs were most effective at 25 mg $L^{-1}$, while ZnO-NPs were equally effective at both 25 and 50 mg $L^{-1}$**.** The findings emphasize the importance of selecting appropriate nanoparticle types and concentrations to maximize benefits while minimizing possible negative effects. These results support the potential application of green-synthesized nanoparticles, particularly in seed priming, to enhance early germination and promote uniform seedling emergence in tomato cultivation.

The effect of *C. fistula*-mediated green-synthesized silver nanoparticles (AgNPs) on seed germination of *Brassica napus* cv. BARI Sarisha-18 was studied at five concentrations: 0, 25, 50, 75, and 100 mg $L^{-1}$ over a 7-day period. No germination was recorded at 0 days after sowing (DAS), confirming uniform seed dormancy prior to treatment. By 3 DAS, germination rates varied substantially across treatments. Seeds treated with 100 mg $L^{-1}$ AgNPs exhibited the highest germination (100%), significantly outperforming the control (average 56.7%). Treatments with 25 mg $L^{-1}$ and 50 mg $L^{-1}$ showed moderate germination (70% and 75%, respectively), while the 75 mg $L^{-1}$ treatment showed slightly reduced germination (65%) (Fig. 4 C).

At 7 DAS, germination percentages increased modestly in most treatments. The 100 mg $L^{-1}$treatment maintained complete germination (100%), while the 25 and 50 mg $L^{-1}$ treatments improved to 85% and 80%, respectively. The 75 mg $L^{-1}$ treatment reached 75%, comparable to the best-performing replicate of the control. However, the control group remained variable, with germination ranging from 55% to 75%, indicating inconsistent performance in the absence of AgNP treatment (Fig. 4 C). These findings indicate a dose-dependent effect of AgNPs on Canola seed germination. The highest concentration (100 mg $L^{-1}$) consistently yielded the most rapid and complete germination, suggesting that *B. napus* can tolerate and potentially benefit from relatively high AgNP exposure. Moderate doses (25–50 mg $L^{-1}$) also improved germination compared to the control but to a lesser extent. The variability and lower performance in the control group may be attributed to the lack of nanoparticle-induced enhancements, such as improved water uptake, metabolic stimulation, or antimicrobial protection. The results suggest that green-synthesized AgNPs - particularly at 100 mg $L^{-1}$ - can significantly improve seed germination in *Brassica napus*, supporting their potential use in seed priming to enhance crop establishment and early seedling vigor.

The effect of *C. fistula*-mediated green-synthesized zinc oxide (ZnO) nanoparticles was also evaluated on *B. napus* seed germination using the same concentration range (0 - 100 mg $L^{-1}$). As with AgNPs, no germination was observed at 0 DAS, confirming initial dormancy. By 3 DAS, clear differences emerged among treatments. The 50 mg $L^{-1}$ ZnO-NP treatment resulted in complete germination (100%), followed by the 25 mg $L^{-1}$ treatment (80%) and the 100 mg $L^{-1}$ treatment (70%). The 75 mg $L^{-1}$ treatment produced moderate germination (65%), while the control group showed the lowest and most variable performance (40% - 70%; average ~56.7%) (Fig. 4 H).

At 7 DAS, the 50 mg $L^{-1}$ treatment retained 100% germination, reinforcing its superior effect. The 25 mg $L^{-1}$treatment remained steady at 80%, while both 75 and 100 mg $L^{-1}$ treatments reached 75% and 70%, respectively. The control group showed limited improvement, ranging from 55% to 75%. These results further underscore a dose-dependent response to ZnO-NPs, with 50 mg $L^{-1}$ identified as the optimal concentration for stimulating rapid and complete germination. This enhancement is likely due to ZnO's role in facilitating water absorption, activating germination enzymes, and promoting early metabolic processes. While higher concentrations (75–100 mg $L^{-1}$) did not significantly inhibit germination, they did not offer additional benefits and may introduce mild stress or metabolic delays.

Green-synthesized ZnO nanoparticles significantly improved seed germination in *Brassica napus*, particularly at 50 mg $L^{-1}$. The findings support the application of ZnO-NP seed priming as an eco-friendly and effective method to improve seed germination uniformity and early crop establishment, provided that nanoparticle concentrations are optimized to avoid inhibitory effects. The influence of *C. fistula*-mediated green-synthesized silver nanoparticles (AgNPs) on the seed germination of *Raphanus sativus* cv. BARI Mula-1 was assessed at concentrations of 0, 25, 50, 75, and 100 mg $L^{-1}$over a 7-day period. No germination occurred at 0 days after sowing (DAS), confirming uniform dormancy across treatments. By 3 DAS, germination rates exhibited considerable variation among treatments. The control group showed high variability, with two replicates achieving 100% germination and one at 60%, averaging 86.7%. The 25 mg $L^{-1}$AgNP treatment produced consistent germination (80%), outperforming the higher AgNP concentrations -50 and 75 mg $L^{-1}$ (each at 70%) -

while the 100 mg $L^{-1}$treatment showed the lowest germination (60%), suggesting potential phytotoxicity at this level (Fig. 4 D).

At 7 DAS, germination increased slightly in the 25 mg $L^{-1}$ treatment (reaching 90%), while the 50, 75, and 100 mg $L^{-1}$ treatments remained unchanged. The control group continued to display inconsistency, with some replicates improving to 90%, and others decreasing, averaging around 80%. This inconsistency contrasted with the stable performance observed in the 25 mg $L^{-1}$ AgNP treatment. These findings highlight a concentration-dependent response to AgNPs in radish seed germination. The 25 mg $L^{-1}$ concentration was the most effective, enhancing both the rate and uniformity of germination, likely due to improved physiological activation without inducing stress. In contrast, higher concentrations (50–100 mg $L^{-1}$) did not provide additional benefits and may have inhibited germination due to nanoparticle-induced oxidative or osmotic stress.

The effect of *C. fistula*-mediated green-synthesized zinc oxide nanoparticles (ZnO-NPs) was also investigated under the same conditions. As with AgNPs, no germination was observed at 0 DAS. By 3 DAS, a rapid increase in germination was observed in all ZnO-NP treatments. Both the 50 and 75 mg $L^{-1}$treatments achieved 100% germination, while the 25 mg $L^{-1}$ treatment followed closely at 90%. The control group exhibited variability similar to that of the AgNP control, with a mean germination rate of 86.7%. The 100 mg $L^{-1}$ treatment resulted in a comparatively lower germination rate of 70%, again indicating potential negative effects at higher nanoparticle levels (Fig. 4 I).

By 7 DAS, the germination rates remained stable, with the 50 and 75 mg $L^{-1}$ treatments maintaining 100% germination. The 25 mg $L^{-1}$ treatment also showed sustained performance at 90%, while the 100 mg $L^{-1}$ treatment showed no improvement, remaining at 70%. Control replicates continued to vary, averaging around 80%. These results demonstrate that ZnO-NPs have a strong positive influence on seed germination at moderate concentrations, particularly 50–75 mg $L^{-1}$. These effects may be due to ZnO-NPs enhancing water uptake, enzymatic activity, and metabolic processes essential for germination. However, at 100 mg $L^{-1}$, the benefits diminished, likely due to stress-induced physiological disruption. Both AgNPs and ZnO-NPs showed potential to enhance seed germination in *Raphanus sativus*, with ZnO-NPs at 50–75 mg $L^{-1}$ being the most effective. AgNPs at 25 mg $L^{-1}$also improved germination consistency, but higher concentrations appeared less beneficial or mildly inhibitory. These findings support the use of green-synthesized nanoparticles as seed priming agents, provided concentrations are carefully optimized to avoid phytotoxic effects.

The application of *C. fistula*-mediated green-synthesized silver (AgNPs) and zinc oxide (ZnO-NPs) nanoparticles significantly influenced the seed germination of *Ipomoea aquatica* (Gima Kalmi), particularly at lower concentrations. Both nanoparticle types demonstrated their peak stimulatory effects at 25 and 50 mg $L^{-1}$, achieving 100% germination by 3 days after sowing (DAS), outperforming or matching the control (90–100%). These results suggest that both AgNPs and ZnO-NPs can accelerate and synchronize germination effectively at moderate concentrations. In contrast, the 75 mg $L^{-1}$AgNP treatment resulted in reduced germination (80%), indicating a potential threshold beyond which AgNPs may induce mild inhibitory effects. The ZnO-NP treatments at 75 and 100 mg $L^{-1}$ maintained high germination rates (90%), similar to the control, without noticeable inhibition—though they did not provide further enhancement compared to the 25–50 mg $L^{-1}$ range.

By 7 DAS, germination rates remained unchanged, confirming that peak germination occurred early and consistently in all nanoparticle-treated seeds, especially at the optimal concentrations. These patterns suggest that both nanoparticles promote early metabolic activation, possibly through improved water uptake, enhanced enzymatic activity, or antimicrobial protection at the seed surface. While both AgNPs and ZnO-NPs were effective in enhancing seed germination, ZnO-NPs showed slightly more consistent performance across all tested concentrations, whereas AgNPs showed a mild decline at the intermediate level (75 mg $L^{-1}$). Thus, 25–50 mg $L^{-1}$ is the optimal rangefor both nanoparticle types, supporting their application in seed priming for fast and uniform germination in leafy vegetables like Gima Kalmi.

### 3.3. Effect of green synthesized Ag-NPs and ZnO-NPs on seedling length

The application of *C. fistula*-mediated green-synthesized silver nanoparticles (AgNPs) significantly influenced the root length of rice seedlings (*Oryza sativa* cv. BRRI dhan29), exhibiting a clear concentration-dependent inhibitory effect. The control group, which received no nanoparticle treatment, recorded the greatest root elongation with an average length of 4.1 cm. In contrast, all AgNP-treated groups demonstrated progressively reduced root growth, with mean lengths decreasing from 2.13 cm at 25 mg $L^{-1}$to 1.07 cm at 50 mg $L^{-1}$, 1.23 cm at 75 mg $L^{-1}$, and 0.93 cm at 100 mg $L^{-1}$. Despite earlier findings showing AgNPs can promote seed germination at certain concentrations, their impact on root development remained consistently negative. This discrepancy suggests that while AgNPs may stimulate initial germinative physiology, they concurrently induce oxidative stress or disrupt hormonal signaling pathways essential for root elongation. The inhibition observed at higher concentrations likely results from the cytotoxic effects of silver ions, which may impair nutrient absorption or cause cellular damage. These findings underscore the importance of carefully optimizing AgNP dosages to maximize germination benefits while safeguarding critical post-germination growth processes, such as root development (Fig. 5A). Similarly, shoot length was also significantly influenced by AgNP exposure, though it followed a more complex and non-linear pattern.

The untreated control group achieved the greatest shoot growth, ranging from 5.3 to 9.5 cm with an average of approximately 7.4 cm. In contrast, AgNP-treated groups generally exhibited reduced shoot lengths, though with some variation across concentrations. At 25 mg $L^{-1}$, shoot length averaged 5.23 cm; at 50 mg $L^{-1}$, values ranged from 4.2 to 5.0 cm. Interestingly, the 75 mg $L^{-1}$treatment showed a slight improvement (~5.5 cm average), possibly reflecting a hormetic or adaptive response.

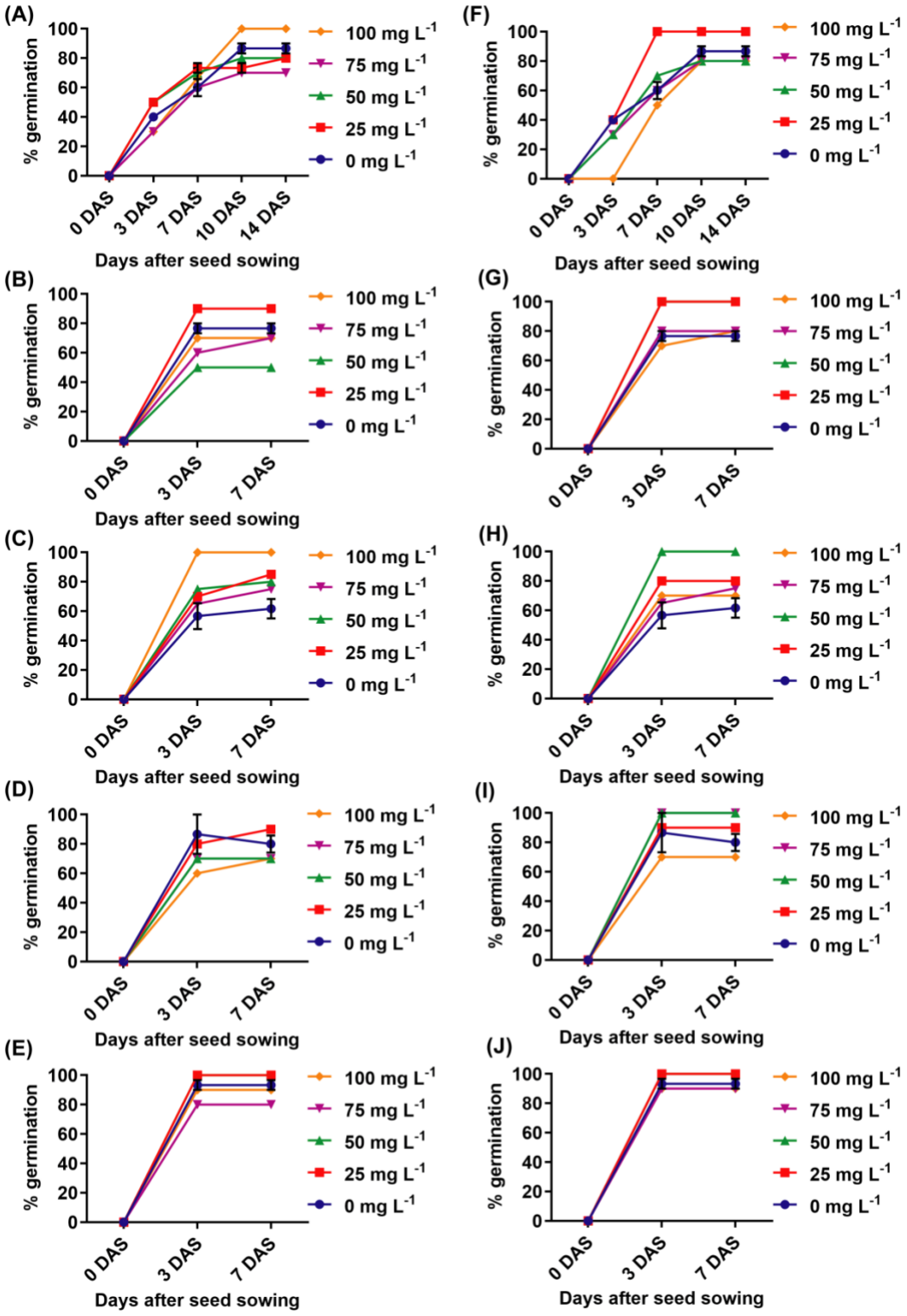


Figure 4. Seed germination (%) of *Oryza sativa* cv. BRRI dhan29 (rice, A and F), *Solanum lycopersicum* cv. BARI Tomato-2 (tomato, B and G), *Brassica napus* cv. BARI Sarisha-18 (canola, C and H), *Raphanus sativus* cv. BARI Mula-1 (radish, D and I), and *Ipomoea aquati*

At 100 mg $L^{-1}$, shoot lengths ranged from 5.3 to 6.2 cm, averaging 5.77 cm—still lower than the control but showing less inhibition than lower concentrations (Fig. 5 A). These patterns indicate that AgNPs may induce early oxidative stress or disrupt elongation-related hormonal pathways at sub-optimal concentrations. The mild recovery at higher concentrations could be due to plant acclimation or activation of internal defense mechanisms. Nevertheless, shoot growth remained consistently lower than control levels, highlighting the delicate balance needed in nanoparticle application to promote seedling vigor without hindering above-ground development.

The effect of *C. fistula*-mediated green-synthesized zinc oxide nanoparticles (ZnO-NPs) on root development also showed a concentration-sensitive response. The control group exhibited relatively greater root lengths (1.5–3.3 cm, average 2.13 cm), while the 25 mg $L^{-1}$ZnO-NP treatment maintained similar performance (mean ~1.9 cm), suggesting a minimal positive effect. However, root length declined sharply with increasing concentrations: to 0.93 cm at 50 mg $L^{-1}$and 0.6 cm at 75 mg $L^{-1}$, with one replicate showing severe inhibition (0.2 cm). At 100 mg $L^{-1}$, root elongation remained inconsistent (0.6–2.0 cm), but generally suppressed compared to the control (Fig. 5 F). These results indicate that while low doses of ZnO-NPs may have a neutral or slightly promotive influence, higher concentrations can exert phytotoxic effects—likely through oxidative stress, metal ion toxicity, or disruption of root cell proliferation and elongation. Thus, ZnO-NPs, like AgNPs, require precise dosage control to avoid detrimental outcomes in early seedling development.

Shoot length responses to ZnO-NP treatment followed a similarly concentration-sensitive trend. The control group recorded the longest shoot lengths (5.3–9.5 cm, average ~7.4 cm). At 25 mg $L^{-1}$, results were mixed, with one replicate achieving 9.3 cm while others dropped to around 4.3–4.6 cm (mean ~6.1 cm). Higher concentrations led to a clear decline: the 50 mg $L^{-1}$ treatment averaged ~4.63 cm, while the 75 mg $L^{-1}$and 100 mg $L^{-1}$treatments showed further reductions to ~3.5 cm and ~3.9 cm, respectively (Fig. 6F). This declining trend with increasing ZnO levels highlights a dose-dependent inhibitory effect on shoot elongation. The occasional outlier at 25 mg $L^{-1}$may reflect experimental variability or individual seedling tolerance. Overall, the results suggest that while ZnO-NPs can support seed germination, their overuse may hinder shoot development due to stress responses, interference with water and nutrient uptake, or hormonal imbalance. This underscores the necessity of careful concentration management in nanoparticle-based agricultural applications, ensuring enhanced germination without compromising post-emergence growth, especially shoot elongation critical for early photosynthetic activity and crop establishment.

The application of *C. fistula*-mediated green-synthesized silver nanoparticles (AgNPs) significantly impacted the root development of *Solanum lycopersicum* cv. BARI Tomato-2, exhibiting a pronounced concentration-dependent inhibitory effect. The control group (0 mg $L^{-1}$) displayed the most vigorous root growth, with lengths ranging from 5.5 to 7.5 cm and a mean of 6.83 cm, indicating optimal root elongation in the absence of nanoparticle interference. However, exposure to AgNPs led to a sharp decline in root length. At 25 mg $L^{-1}$, the average root length dropped dramatically to approximately 1.1 cm, suggesting early phytotoxic effects even at low concentrations. A modest recovery was observed at 50 mg $L^{-1}$ (mean ~2.43 cm), but the values remained significantly lower than the control. A further reduction occurred at 75 mg $L^{-1}$ (mean ~1.43 cm), and while a slight increase was noted at 100 mg $L^{-1}$ (mean ~2.0 cm), root elongation never approached control levels (Fig. 5B). This pattern highlights the high sensitivity of tomato roots to AgNP exposure. The drastic inhibition at 25 mg $L^{-1}$suggests that AgNPs may interfere with root cell division or elongation by inducing oxidative stress, disrupting auxin transport, or releasing phytotoxic silver ions. Although the partial recovery at higher concentrations could suggest physiological adaptation or activation of defense mechanisms, root development remained substantially impaired. These findings underscore the need for careful calibration of AgNP dosage in tomato cultivation, as both sub-lethal and excessive concentrations can compromise early root architecture, essential for water and nutrient uptake.

Shoot development was similarly affected by AgNP treatment, with *Solanum lycopersicum* seedlings showing a consistent decline in shoot elongation as nanoparticle concentration increased. The control group exhibited the highest shoot lengths (2.0–2.5 cm; mean ~2.17 cm). At 25 mg $L^{-1}$, shoot growth remained comparable (mean ~2.0 cm), suggesting a threshold effect where minor exposure does not trigger stress responses. However, at 50 mg $L^{-1}$, mean shoot length declined to ~1.5 cm, and both 75 and 100 mg $L^{-1}$ treatments showed further suppression, with average values around 1.17 cm (Fig. 6B).This consistent decrease indicates a dose-dependent phytotoxic effect likely stemming from oxidative stress, hormonal imbalances (particularly involving auxins or gibberellins), or impaired vascular function. The alignment between root and shoot responses confirms that tomato seedlings are particularly vulnerable to silver nanoparticle exposure during early development. Although AgNPs may offer benefits for pathogen control or germination in other systems, their detrimental impact on subsequent seedling growth in tomato highlights the importance of crop-specific nanoparticle assessment.

In contrast, the effect of *Cassia fistula*-mediated green-synthesized zinc oxide nanoparticles (ZnO-NPs) on tomato root length revealed a more variable, yet still largely inhibitory, response. The control group once again exhibited superior root elongation (5.5–7.5 cm; mean ~6.83 cm). At 25 mg $L^{-1}$, root lengths ranged from 2.0 to 4.0 cm (mean ~2.83 cm), indicating a substantial reduction. Similar results were observed at 50 mg $L^{-1}$(mean ~2.77 cm), although variability was slightly higher. A noteworthy anomaly occurred at 75 mg $L^{-1}$, where one replicate reached 6.8 cm—approaching control levels—raising the possibility of hormesis or experimental variability. Despite this, the average root length remained lower (mean ~4.1 cm), and at 100 mg $L^{-1}$, consistent suppression was observed (2.0–2.5 cm; mean ~2.33 cm) (Fig. 5G). These observations suggest that while ZnO-NPs may not be as severely phytotoxic as AgNPs at equivalent concentrations, they still induce stress responses that hinder root elongation. The reduction is likely due to ZnO-NP-induced oxidative stress, interference with cellular expansion, or nanoparticle aggregation around root surfaces, limiting nutrient and water absorption. The variable response at intermediate

concentrations further emphasizes the need for precision in dosing.

Shoot length under ZnO-NP treatment was less affected, showing only subtle differences across concentrations. The control group maintained the highest mean shoot length (~2.17 cm), with 25 mg $L^{-1}$ producing comparable results. A slight, non-significant increase occurred at 50 mg $L^{-1}$(mean ~2.33 cm), and 75 mg $L^{-1}$ showed a modest uptick with one outlier reaching 2.8 cm (mean ~2.27 cm). However, at 100 mg $L^{-1}$, shoot growth declined slightly again (mean ~2.0 cm) (Fig. 6G). These mild fluctuations suggest that ZnO-NPs, unlike AgNPs, do not drastically inhibit shoot development in tomato, at least within the tested concentration range. Nevertheless, the absence of notable improvement beyond control levels indicates limited benefit for shoot elongation, even at optimized doses.

The results demonstrate that both AgNPs and ZnO-NPs affect tomato seedling development in a concentration-dependent manner, with roots being more sensitive than shoots. Silver nanoparticles exhibited stronger phytotoxic effects, particularly at lower doses, whereas zinc oxide nanoparticles caused milder, yet still notable, growth inhibition at higher concentrations. These findings emphasize the need for species-specific and development-stage-specific guidelines when applying green-synthesized nanoparticles in agriculture. While nanoparticle priming may enhance germination in some contexts, careful calibration is essential to prevent adverse effects on early vegetative growth—especially in sensitive crops like tomato.

The study evaluated the impact of *C. fistula*-mediated green-synthesized silver (Ag) and zinc oxide (ZnO) nanoparticles on the root and shoot growth of *Brassica napus* cv. BARI Sarisha-18 seedlings. Results revealed concentration-dependent and nanoparticle-specific effects on both root and shoot development. For Ag nanoparticles, root length exhibited variable responses. The control group (0 mg $L^{-1}$) had the highest mean root length (6.23 cm), closely followed by 50 mg $L^{-1}$(6.10 cm), indicating minimal inhibition at moderate concentrations. In contrast, root length significantly declined at 75 mg $L^{-1}$(4.53 cm) and 100 mg $L^{-1}$(3.30 cm), suggesting a dose-dependent phytotoxic effect. Interestingly, the 25 mg $L^{-1}$group displayed high variability, with one replicate reaching 12 cm, potentially due to experimental variation or uneven nanoparticle uptake (Fig. 5C). Shoot growth under Ag NPs followed a similar pattern. While control seedlings averaged 2.3 cm, a slight increase was noted at 25 mg $L^{-1}$(2.5 cm), suggesting possible stimulation at low concentrations. Shoot length remained stable at 50 mg $L^{-1}$(~2.4 cm) but declined markedly at 75 mg $L^{-1}$ (2.2 cm) and 100 mg $L^{-1}$ (1.4 cm), indicating that higher Ag NP concentrations hinder shoot elongation, likely due to oxidative stress or nutrient interference (Fig. 6C).

ZnO nanoparticles, in contrast, showed a general trend of growth suppression with increasing concentration. Root length was highest in the control group (6.23 cm) and decreased steadily across treatments: 4.3 cm at 25 mg $L^{-1}$, 3.9 cm at 50 mg $L^{-1}$, 3.7 cm at 75 mg $L^{-1}$, and only 2.03 cm at 100 mg $L^{-1}$ (Fig. 5H). These results indicate a clear concentration-dependent inhibitory effect, likely due to stress on root cell division or elongation processes. Shoot length under ZnO exposure also demonstrated variability. The control group had an average of 2.3 cm, which declined to 2.0 cm at 25 mg $L^{-1}$and further to 1.7 cm at 50 mg $L^{-1}$. A slight rebound was observed at 75 mg $L^{-1}$(2.23 cm), possibly reflecting transient tolerance or adaptive response, but shoot length dropped again at 100 mg $L^{-1}$(1.77 cm), indicating toxic stress at higher nanoparticle levels (Fig. 6H).

Both Ag and ZnO nanoparticles influenced seedling development in *B. napus* in a dose-dependent manner. Lower concentrations appeared relatively safe or mildly beneficial, while higher concentrations led to reduced root and shoot growth. These findings underscore the importance of careful dose regulation when considering the use of green-synthesized nanoparticles in agricultural practices. The growth response of *Raphanus sativus* cv. BARI Mula-1 seedlings to *C. fistula*-mediated green-synthesized silver (Ag) and zinc oxide (ZnO) nanoparticles revealed significant, dose-dependent effects on both root and shoot development.

Root length responded variably to Ag NP exposure. The control group showed a moderate average root length of 3.73 cm. A slight increase to 4.33 cm was observed at 25 mg $L^{-1}$, suggesting a mild stimulatory effect at low concentrations. However, root length declined at 50 mg $L^{-1}$ (mean: 2.6 cm) and further at 100 mg $L^{-1}$ (mean: 2.3 cm), indicating phytotoxicity at elevated levels. Interestingly, root length at 75 mg $L^{-1}$ showed wide variability (0.5–7.5 cm), possibly due to inconsistent nanoparticle absorption or differential seedling sensitivity (Fig. 5D).

Shoot growth under Ag NP treatment exhibited a stronger and more consistent inhibitory pattern. Control seedlings had the highest mean shoot length (8.57 cm), but exposure to even 25 mg $L^{-1}$ led to a sharp decrease (mean: 2.13 cm), highlighting early onset of phytotoxicity. Though a slight recovery was noted at 50 mg $L^{-1}$ (3.27 cm), further increases in concentration resulted in reduced shoot length—1.67 cm at 75 mg $L^{-1}$ and 2.73 cm at 100 mg $L^{-1}$ (Fig. 6D). These findings underscore the high sensitivity of *R. sativus* shoots to Ag NPs, with potential mechanisms of toxicity including oxidative stress, impaired water/nutrient uptake, and disruption of cellular functions.

In case of Zinc Oxide nanoparticles (ZnO NPs), root growth showed a biphasic response. While the control group had a mean root length of 3.73 cm, exposure to 25 mg $L^{-1}$ significantly enhanced root elongation (mean: 6.27 cm), likely due to zinc's known role in promoting cell division and enzymatic activity. However, higher concentrations progressively suppressed root growth: 2.17 cm at 50 mg $L^{-1}$, 0.83 cm at 75 mg $L^{-1}$, and 1.07 cm at 100 mg $L^{-1}$, with some seedlings exhibiting extreme reductions (as low as 0.2 cm) (Fig. 5I). This demonstrates that ZnO NPs promote growth only at low doses, beyond which toxicity dominates. Shoot growth followed a similar trend. Control plants averaged 8.57 cm in shoot length. At 25 mg $L^{-1}$, shoot growth remained relatively robust (mean: ~7.0 cm), but declined steadily at higher concentrations: 5.07 cm at 50 mg $L^{-1}$, 2.17 cm at 75 mg $L^{-1}$, and 3.8 cm at 100 mg $L^{-1}$ (Fig. 6I). The initial stimulatory effect likely results from essential micronutrient activity of zinc, while the suppression at higher concentrations may stem from nanoparticle-induced oxidative stress or hormonal disruption.

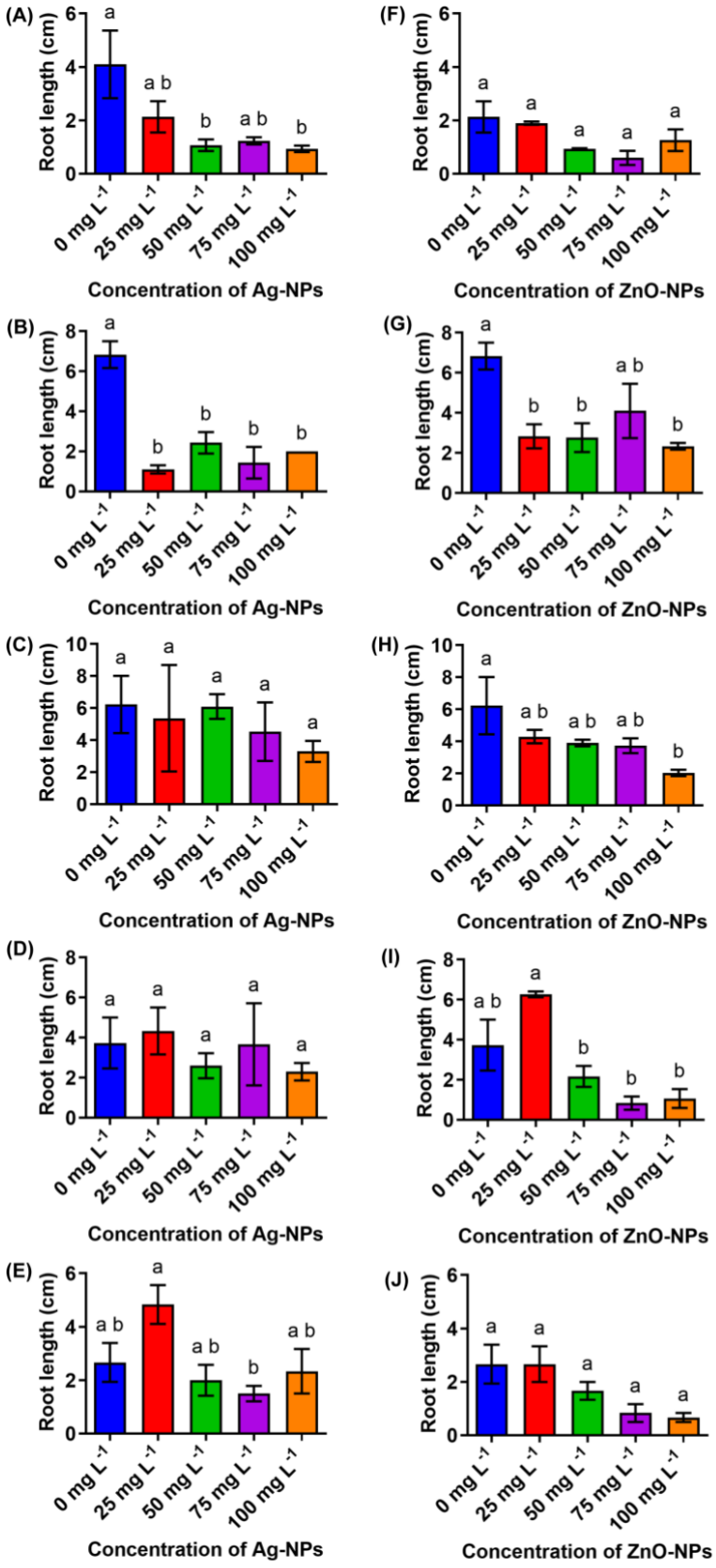


Figure 5. Seedling root length of *Oryza sativa* cv. BRRI dhan29 (rice, A and F), *Solanum lycopersicum* cv. BARI Tomato-2 (tomato, B and G), *Brassica napus* cv. BARI Sarisha-18 (canola, C and H), *Raphanus sativus* cv. BARI Mula-1 (radish, D and I), and *Ipomoea aquatica* cv. Gima kalmi (water spinach, E and J)—as influenced by *Cassia fistula*-mediated green-synthesized silver (Ag) nanoparticles (A–E) and zinc oxide (ZnO) nanoparticles (F–J). Error bars represent the variability of data. Bars sharing the same letter (e.g., "a" vs. "a") are not significantly different from each other

Both Ag and ZnO nanoparticles influenced seedling growth in *R. sativus* in a dose-dependent manner. Low concentrations, particularly of ZnO NPs, showed growth-promoting effects on roots and shoots, while higher concentrations of both nanoparticles inhibited development. These findings highlight the potential of green-synthesized nanoparticles as agricultural tools but also emphasize the importance of dosage control to avoid phytotoxicity.

The root growth of *Ipomoea aquatica* cv. Gima Kalmi exhibited variable responses to different concentrations of *C. fistula*-mediated green-synthesized silver nanoparticles (Ag NPs). In the control group (0 mg $L^{-1}$), root lengths ranged from 1.5 to 4.0 cm, with an average of approximately 2.67 cm. At 25 mg $L^{-1}$, root elongation increased notably, ranging from 3.5 to 6.0 cm with a mean of about 4.83 cm, suggesting a stimulatory effect at low Ag NP concentrations. However, this positive trend diminished at higher concentrations: root growth decreased significantly at 50 mg $L^{-1}$ (mean ~2.0 cm) and further at 75 mg $L^{-1}$ (mean ~1.5 cm). At 100 mg $L^{-1}$, results were variable, with one replicate reaching 4.0 cm but an overall mean remaining low (~2.33 cm), indicating limited recovery (Fig. 5E). These results imply that while low levels of Ag NPs may promote root growth, higher concentrations are phytotoxic—likely due to oxidative damage, nanoparticle accumulation, or metabolic disruption in root tissues. This highlights the critical need for concentration control in agricultural nanoparticle applications.

Shoot length in *I. aquatica* showed relatively stable and tolerant responses to Ag NP exposure. Control shoots ranged from 5.0 to 6.5 cm, averaging 5.67 cm. At 25 mg $L^{-1}$, a slight reduction to 3.83 cm mean suggested mild stress, but shoot length recovered at 50 mg $L^{-1}$ (mean ~5.67 cm), similar to control. At 75 mg $L^{-1}$, mean shoot length was 4.17 cm, indicating moderate tolerance or adaptation, and at 100 mg $L^{-1}$, shoots remained robust (mean ~5.0 cm) without significant phytotoxicity (Fig. 6E). This contrast with root sensitivity may be due to differential nanoparticle uptake or enhanced detoxification in aerial tissues.

Root growth under Cassia fistula-mediated green-synthesized zinc oxide (ZnO) nanoparticles exhibited a clear dose-dependent inhibition.Control root lengths averaged 2.67 cm. At 25 mg $L^{-1}$, roots remained comparable to control (mean ~2.67 cm), but root length declined sharply at 50 mg $L^{-1}$ (~1.67 cm), further dropping at 75 mg $L^{-1}$ (~0.83 cm) and 100 mg $L^{-1}$ (~0.67 cm) (Fig. 5J). This progressive suppression likely stems from nanoparticle accumulation causing oxidative stress, interfering with cell division and nutrient uptake. These findings underscore that higher ZnO NP concentrations are detrimental to *I. aquatica* root development. In contrast, shoot length demonstrated relative resilience to ZnO nanoparticles. Control shoot length averaged 5.67 cm. At 25 and 50 mg $L^{-1}$, shoot length remained steady (~5.17–5.33 cm). A decline was noted at 75 mg $L^{-1}$ (~3.5 cm), suggesting some phytotoxicity, but at 100 mg $L^{-1}$, shoot length increased again (~4.5 cm), possibly reflecting physiological adaptation or recovery (Fig. 6J). Overall, shoot tissues appear less sensitive to ZnO NPs than roots, likely due to differences in nanoparticle translocation or detoxification mechanisms.

### 3.4. Effect of green synthesized Ag-NPs and ZnO-NPs on seedling weight

The seedling weight of *Oryza sativa* cv. BRRI dhan29 was significantly affected by varying concentrations of *C. fistula*-mediated green-synthesized silver (Ag) and zinc oxide (ZnO) nanoparticles. In both cases, the control treatment (0 mg $L^{-1}$) produced the highest mean seedling weight (0.072 g), indicating optimal growth in the absence of nanoparticles (Fig. 7A and 7F).

For silver nanoparticles, a gradual decline in seedling biomass was observed with increasing concentrations. At 25 mg $L^{-1}$, the mean seedling weight slightly decreased to 0.064 g, followed by a further reduction to 0.054 g at 50 mg $L^{-1}$. Interestingly, a plateau effect occurred at higher concentrations: both 75 mg $L^{-1}$ and 100 mg $L^{-1}$ showed a nearly identical mean seedling weight of 0.056 g (Fig. 7A). This trend suggests a potential toxicity threshold beyond which additional nanoparticle exposure did not significantly worsen plant growth. The reduction in biomass at higher Ag nanoparticle concentrations is consistent with reported phytotoxic effects of metallic nanoparticles, potentially due to oxidative stress, disruption of cell membranes, or inhibition of essential metabolic processes. The minor rebound at higher doses may reflect either experimental variability or a physiological adaptation mechanism in the seedlings.

In the case of ZnO nanoparticles, a similar concentration-dependent response was evident but with more pronounced phytotoxicity at higher doses. At 25 mg $L^{-1}$, the mean seedling weight slightly declined to 0.066 g, indicating minimal stress. However, seedling weight dropped more sharply at 50 mg $L^{-1}$ (0.057 g) and dramatically decreased to 0.038 g at 75 mg $L^{-1}$, suggesting significant growth inhibition. A slight improvement was noted at 100 mg $L^{-1}$ (0.057 g), though values remained lower than the control (Fig. 7F). These results point to heightened sensitivity of rice seedlings to ZnO nanoparticles, possibly due to enhanced oxidative stress or nanoparticle interference with nutrient uptake and hormonal balance. Both types of green-synthesized nanoparticles negatively affected seedling weight at higher concentrations, with ZnO showing a more acute inhibitory effect compared to Ag. These findings are in line with existing literature on nanoparticle phytotoxicity and highlight the importance of dose optimization when considering the use of nanomaterials in agriculture. While low concentrations (≤25 mg $L^{-1}$) showed limited impact, higher doses significantly reduced biomass accumulation, indicating the need for cautious application to avoid compromising early seedling development. The seedling weight of *Solanum lycopersicum* cv. BARI Tomato-2 responded sensitively to increasing concentrations of *Cassia fistula*-mediated green-synthesized silver (Ag) and zinc oxide (ZnO) nanoparticles, with both treatments inducing a dose-dependent decline in biomass. For Ag nanoparticles, the control group (0 mg $L^{-1}$) recorded the highest mean seedling weight (0.038 g), indicating optimal growth in nanoparticle-free conditions. At 25 mg $L^{-1}$, seedling weight dropped markedly to 0.027 g, and declined even further to 0.014 g at 50 mg $L^{-1}$. The lowest mean weight was recorded at 75 mg $L^{-1}$ (0.013 g), followed by a slight increase at 100 mg $L^{-1}$ (0.017 g) (Fig. 7B).

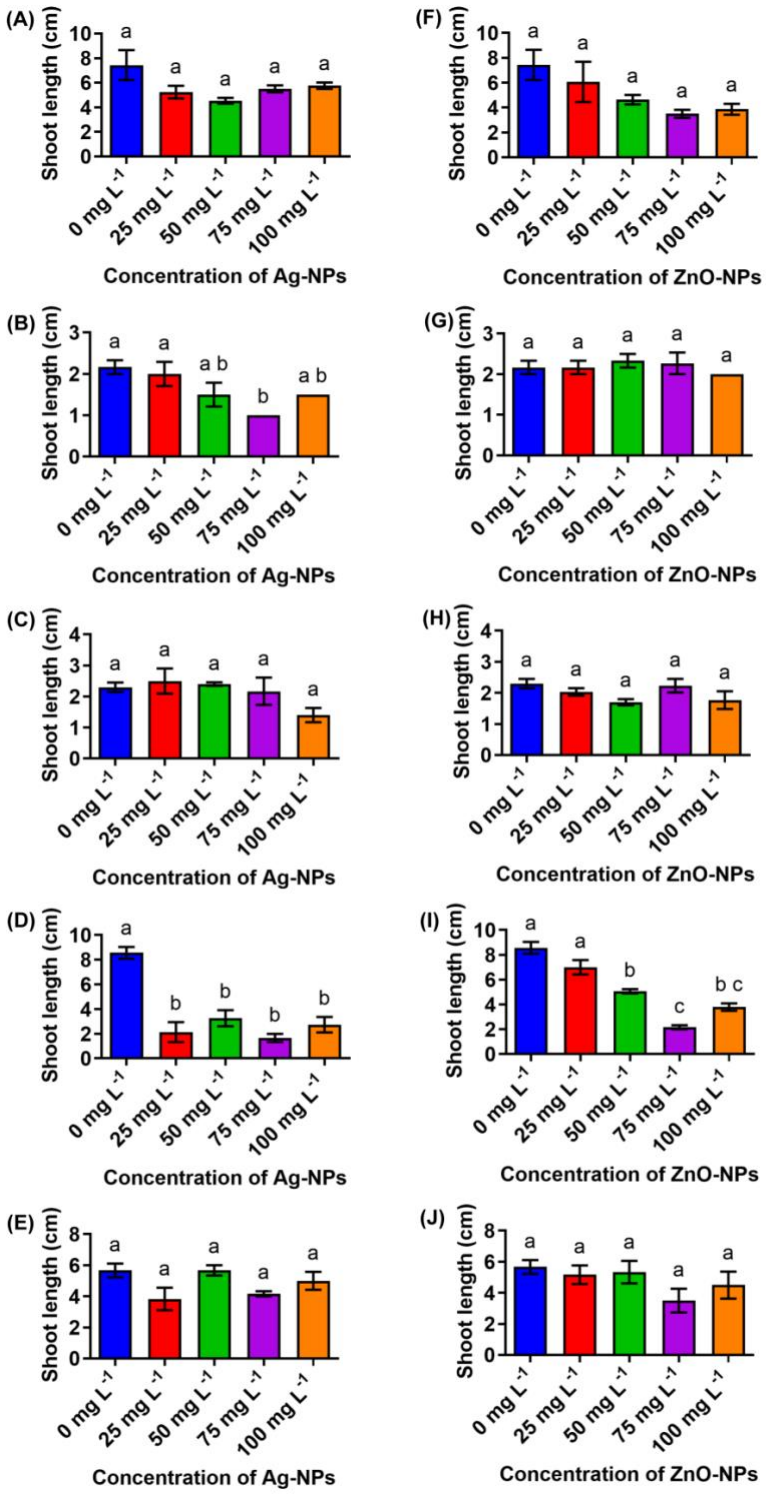


Figure 6. Seedling shoot length of *Oryza sativa* cv. BRRI dhan29 (rice, A and F), *Solanum lycopersicum* cv. BARI Tomato-2 (tomato, B and G), *Brassica napus* cv. BARI Sarisha-18 (canola, C and H), *Raphanus sativus* cv. BARI Mula-1 (radish, D and I), and *Ipomoea aquatica* cv. Gima kalmi (water spinach, E and J)—as influenced by *Cassia fistula*-mediated green-synthesized silver (Ag) nanoparticles (A–E) and zinc oxide (ZnO) nanoparticles (F–J). Error bars represent the variability of data. Bars sharing the same letter (e.g., "a" vs. "a") are not significantly different from each other

This consistent downward trend highlights a strong phytotoxic response of tomato seedlings to Ag nanoparticles, likely driven by oxidative stress, membrane damage, or disruption of root morphology. The modest rebound at the highest dose may reflect a stress-adaptive metabolic shift or experimental variability. Similarly, ZnO nanoparticle treatments also resulted in a decline in seedling biomass. The control group maintained the highest average seedling weight (0.038 g), while 25 mg $L^{-1}$showed a minor reduction to 0.032 g. At 50 mg $L^{-1}$, weight decreased more significantly to 0.023 g, but a slight increase was observed at 75 mg $L^{-1}$ (0.027 g). Seedlings treated with 100 mg $L^{-1}$ ZnO nanoparticles showed a final drop to 0.017 g. While ZnO exhibited a broadly similar phytotoxic pattern to Ag, the reduction in seedling weight appeared less abrupt at moderate concentrations. This suggests that ZnO nanoparticles may be comparatively less toxic than Ag nanoparticles, particularly in the 25–75 mg $L^{-1}$ range (Fig. 7G).

Both nanoparticle types negatively impacted tomato seedling development beyond 25 mg $L^{-1}$, underscoring their phytotoxic potential. Ag nanoparticles exhibited a more pronounced inhibitory effect, while ZnO nanoparticles showed a slightly more variable but still downward trend in seedling biomass. These results align with existing literature indicating that while green-synthesized nanoparticles can offer agricultural benefits at low doses, their excessive application may suppress plant growth through stress-related mechanisms(Batool *et al.*, 2024; Kilic *et al.*, 2025). Careful dose regulation and further mechanistic studies are warranted before such nanomaterials are adopted for widespread agronomic use, especially for sensitive crops like tomato.

The seedling weight of *Brassica napus* cv. BARI Sarisha-18 exhibited a non-linear, biphasic response to different concentrations of *C. fistula*-mediated green-synthesized silver (Ag) nanoparticles. The control treatment (0 mg $L^{-1}$) showed an average seedling weight of 0.077 g, reflecting normal growth without nanoparticle stress. At 25 mg $L^{-1}$, the seedling weight slightly decreased to 0.068 g, indicating mild phytotoxicity. Interestingly, an increase was observed at 50 mg $L^{-1}$, where the mean seedling weight peaked at 0.089 g, suggesting a stimulatory effect of Ag nanoparticles at moderate concentration. At 75 mg $L^{-1}$, seedling weights showed high variability (0.041–0.131 g), averaging 0.087 g. However, at the highest concentration (100 mg $L^{-1}$), seedling weight sharply declined to 0.029 g, signifying clear phytotoxic effects likely due to oxidative stress, cellular toxicity, or inhibited nutrient uptake (Fig. 7C).

This hormetic dose-response, characterized by growth promotion at moderate doses followed by toxicity at higher levels, is consistent with previous studies on nanoparticle–plant interactions. It underscores the need to identify optimal nanoparticle concentrations to maximize benefits while minimizing harm in agricultural applications. In contrast, the seedling weight of *Brassica napus* was consistently reduced with increasing concentrations of *C. fistula*-mediated green-synthesized zinc oxide (ZnO) nanoparticles, showing a clear dose-dependent toxicity. The control group had the highest mean seedling weight of 0.077 g. At 25 mg $L^{-1}$, the weight declined slightly to 0.061 g, followed by a gradual decrease at 50 mg $L^{-1}$ (0.059 g) and 75 mg $L^{-1}$ (0.060 g), although variability was observed. The most significant reduction occurred at 100 mg $L^{-1}$, where seedling weight dropped to 0.033 g, less than half of the control (Fig. 7H). The gradual decline with ZnO nanoparticles suggests oxidative stress, cellular damage, and interference with nutrient uptake and hormonal regulation as probable causes of reduced growth. Compared to Ag nanoparticles, ZnO nanoparticles showed a more consistent inhibitory effect, albeit less abrupt until the highest concentration. This may indicate better tolerance of *B. napus* to ZnO stress at intermediate levels but clear toxicity at excessive doses. These findings emphasize the importance of dose optimization when applying green-synthesized nanoparticles in crop management. While low to moderate doses of Ag nanoparticles might stimulate growth, both Ag and ZnO nanoparticles exhibit phytotoxicity at high concentrations, which could hinder seedling development and crop productivity.

The seedling weight of *Raphanus sativus* cv. BARI Mula-1 was significantly affected by varying concentrations of *C. fistula*-mediated green-synthesized silver (Ag) nanoparticles, exhibiting a clear inhibitory trend with increasing nanoparticle levels. The control group (0 mg $L^{-1}$) showed the highest and most variable seedling weights, ranging from 0.221 to 0.429 g, with an average of approximately 0.333 g, indicating healthy growth without nanoparticle-induced stress. At 25 mg $L^{-1}$, seedling weight drastically decreased to an average of 0.067 g (range: 0.040–0.105 g), demonstrating strong phytotoxicity even at low concentrations. A partial recovery was observed at 50 mg $L^{-1}$ (mean ~0.14 g), though variability persisted, with values between 0.077 and 0.238 g, suggesting inconsistent seedling responses potentially due to differential tolerance or nanoparticle uptake. At higher concentrations of 75 mg $L^{-1}$ and100 mg $L^{-1}$, seedling biomass remained suppressed, averaging approximately 0.057 g and 0.072 g respectively, significantly lower than control seedlings (Fig. 7D). This sustained reduction likely results from oxidative stress, cellular toxicity, and disruption of water and nutrient uptake caused by silver nanoparticles. These findings highlight the high sensitivity of radish seedlings to Ag nanoparticles and underscore the need for cautious concentration management in agricultural applications to avoid adverse effects on sensitive crops.

Similarly, the seedling weight of *Raphanus sativus* cv. BARI Mula-1 was influenced by *C. fistula*-mediated green-synthesized zinc oxide (ZnO) nanoparticles, showing a dose-dependent decline. Control seedlings exhibited the highest biomass (average ~0.333 g), with values ranging from 0.221 to 0.429 g. At 25 mg $L^{-1}$ZnO, seedling weight remained relatively high (mean ~0.251 g), suggesting minimal phytotoxic effects at low doses. However, biomass declined at 50 mg $L^{-1}$ (~0.170 g) and decreased more sharply at 75 mg $L^{-1}$ (~0.065 g), indicating progressive growth inhibition. Interestingly, at 100 mg $L^{-1}$, a partial recovery was noted (mean ~0.126 g), although weights remained below control levels, possibly reflecting adaptive physiological responses or experimental variability (Fig. 7I). These results suggest that ZnO nanoparticles induce concentration-dependent phytotoxicity in radish seedlings, likely through oxidative stress, membrane disruption, and interference with nutrient uptake. Compared to Ag nanoparticles, ZnO appears less immediately toxic at lower concentrations but still adversely affects seedling growth at higher doses.

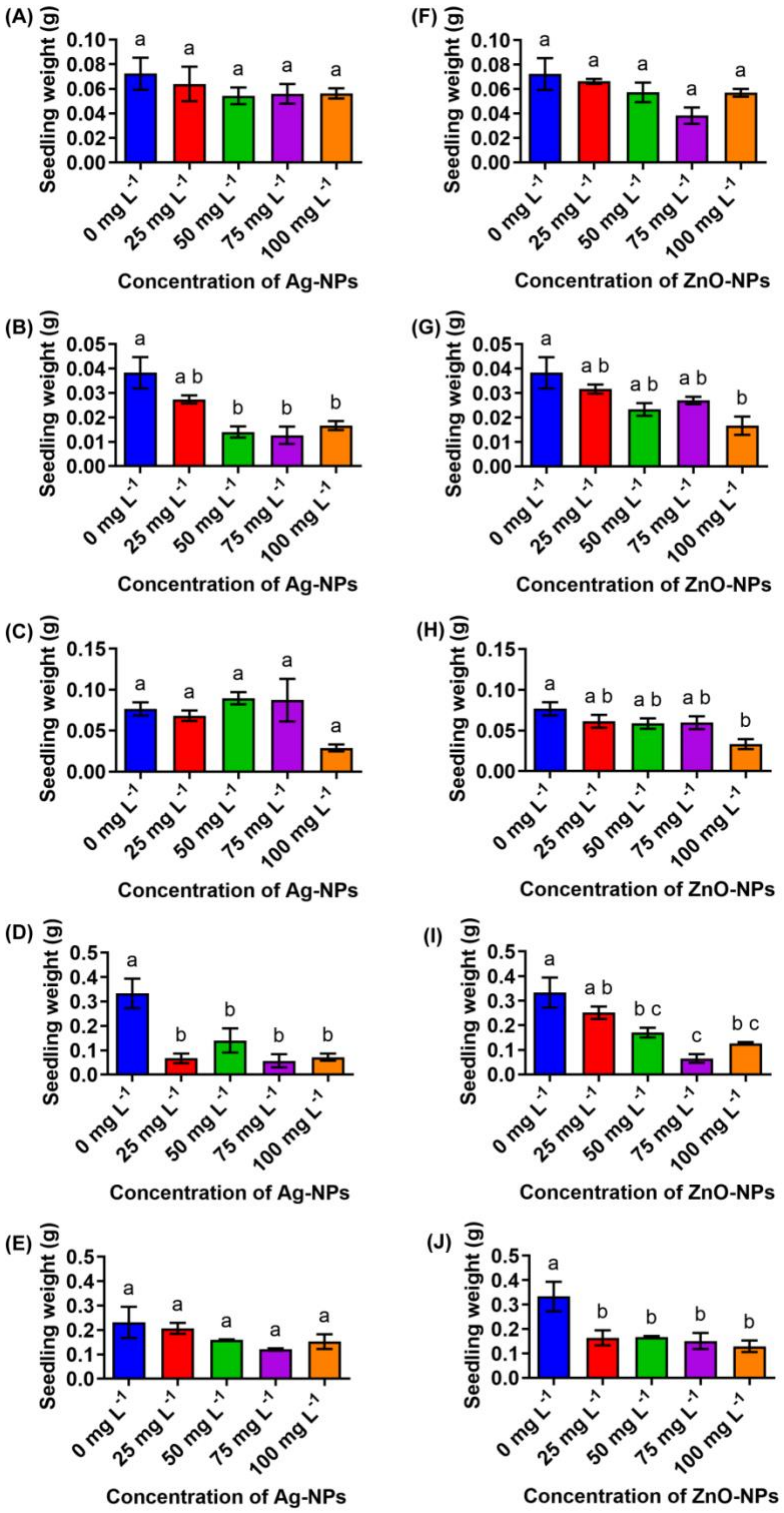


Figure 7. Seedling weight of *Oryza sativa* cv. BRRI dhan29 (rice, A and F), *Solanum lycopersicum* cv. BARI Tomato-2 (tomato, B and G), *Brassica napus* cv. BARI Sarisha-18 (canola, C and H), *Raphanus sativus* cv. BARI Mula-1 (radish, D and I), and *Ipomoea aquatica* cv. Gima kalmi (water spinach, E and J)—as influenced by *Cassia fistula*-mediated green-synthesized silver (Ag) nanoparticles (A–E) and zinc oxide (ZnO) nanoparticles (F–J). Error bars represent the variability of data. Bars sharing the same letter (e.g., "a" vs. "a") are not significantly different from each other

Collectively, these findings emphasize the importance of precise dosage control for ZnO nanoparticles to harness their potential benefits while minimizing risks to early seedling development in sensitive crops like radish. The seedling weight of *Ipomoea aquatica* cv. Gima kalmi was influenced by varying concentrations of *C. fistula*-mediated green-synthesized silver (Ag) nanoparticles, exhibiting a general decline in biomass with increasing nanoparticle levels, although some variability was observed. The control group (0 mg $L^{-1}$) showed the highest and most consistent seedling weights, ranging from 0.105 to 0.307 g, with a mean of approximately 0.231 g, indicating healthy growth without nanoparticle stress. At 25 mg $L^{-1}$, seedling weight moderately decreased to an average of 0.206 g, suggesting mild phytotoxicity. Further increases to 50 mg $L^{-1}$ resulted in a more pronounced decline, with an average of 0.159 g, indicating stronger growth inhibition. At 75 mg $L^{-1}$, mean seedling weight dropped further to about 0.120 g with low variability, reflecting clear phytotoxic effects. Interestingly, at 100 mg $L^{-1}$, seedling weight partially recovered to around 0.152 g, though still below control levels, possibly due to adaptive physiological responses or experimental variation. Overall, these results suggest a dose-dependent inhibitory effect of Ag nanoparticles on seedling growth, likely driven by oxidative stress and cellular toxicity(Fig. 7E).

Similarly, seedling weight was affected by *C. fistula*-mediated green-synthesized zinc oxide (ZnO) nanoparticles, showing a variable yet generally declining trend with increasing concentrations. Control seedlings (0 mg $L^{-1}$) exhibited the highest and most variable biomass, ranging from 0.221 to 0.429 g, with a mean of approximately 0.333 g. At 25 mg $L^{-1}$ ZnO, seedling weight decreased slightly to about 0.164 g, indicating mild stress. At 50 mg $L^{-1}$, biomass remained relatively stable (mean ~0.168 g), suggesting moderate ZnO levels may not exacerbate toxicity significantly. The 75 mg $L^{-1}$ treatment showed increased variability and a slight decline (mean ~0.151 g), while at 100 mg $L^{-1}$, seedling weight further decreased to a mean of approximately 0.129 g, indicating moderate inhibition compared to controls (Fig. 7J). The observed biomass reduction is likely related to ZnO nanoparticle-induced oxidative stress and disruption of cellular functions. These findings are consistent with previous studies reporting dose-dependent phytotoxicity of metal oxide nanoparticles in aquatic plants, underscoring the need for careful concentration optimization to balance potential benefits with phytotoxic risks.

## 4. Conclusion

The study successfully demonstrated the green synthesis of silver (Ag-NPs) and zinc oxide (ZnO-NPs) nanoparticles using *C. fistula* leaf extract and characterized their formation through UV-Vis spectroscopy and energy band gap analysis. The biological effects of these nanoparticles on seed germination, seedling growth, and biomass of various crops showed clear concentration-dependent responses. Optimal low to moderate nanoparticle concentrations enhanced seed germination and early growth in species such as rice, tomato, mustard, radish, and water spinach, while higher doses caused delayed germination, growth inhibition, and phytotoxicity, particularly with Ag-NPs. Root growth was generally more sensitive than shoots, and Ag-NPs exhibited stronger toxicity than ZnO-NPs, likely due to oxidative stress and ion toxicity. Seedling biomass declined dose-dependently under nanoparticle treatment, emphasizing that while green-synthesized nanoparticles have potential as growth enhancers, careful dosage optimization is critical to avoid adverse effects and maximize agricultural benefits.


## Acknowledgement

The authors gratefully acknowledge the National Science and Technology (NST) Fellowship provided by the Ministry of Science and Technology, Government of the People's Republic of Bangladesh, to the first four author. The authors also extend their sincere thanks to the Bangladesh Agricultural University Research System (BAURES) for providing comprehensive financial and logistical support, which was essential for the successful completion of this research.


## Conflict of Interests

The authors declare that there is no conflict of interests regarding the publication of this paper.

## References


Aslani, F., Bagheri, S., MuhdJulkapli, N., Juraimi, A.S., Hashemi, F.S.G. and Baghdadi, A. 2014. Effects of engineered nanomaterials on plants growth: an overview. The Scientific World Journal, 2014. https://doi.org/10.1155/2014/641759

Aziz, A., Khalid, M., Saeed Akhtar, M., Nadeem, M., Gilani, Z., Khan, M., Rehman, J., Ullah, Z. and Saleem, M. 2018. Structural, morphological and optical investigations of silver nanoparticles synthesized by sol-gel auto-combustion method. 13: 679-683.

Batool, F., Hassan, S., Zulfiqar, H.F., Shakoor, S., Afroze, B., Bhutta, M.S., Ahmed, M. and Rashid, B. 2024. Nanoparticles in Agriculture: Enhancing Crop Resilience and Productivity against Abiotic Stresses, In: Hasanuzzaman, M. and Nahar, K. (Eds.), Abiotic Stress in Crop Plants - Ecophysiological Responses and Molecular Approaches. IntechOpen, Rijeka. https://doi.org/10.5772/intechopen.114843

Bayat, M., Zargar, M., Murtazova, K., Nakhaev, M. and Shkurkin, S. 2022. Ameliorating Seed Germination and Seedling Growth of Nano-Primed Wheat and Flax Seeds Using Seven Biogenic Metal-Based Nanoparticles. Agronomy, 12: 811. https://doi.org/10.3390/agronomy12040811

Brus, L. 1986. Electronic wave functions in semiconductor clusters: experiment and theory. The Journal of Physical Chemistry, 90(12): 2555-2560. https://doi.org/10.1021/j100403a003

Chand Mali, S., Raj, S. and Trivedi, R. 2020. Nanotechnology a novel approach to enhance crop productivity. BiochemBiophys Rep, 24: 100821.

https://doi.org/10.1016/j.bbrep.2020.100821

Faisal, S., Jan, H., Shah, S.A., Shah, S., Khan, A., Akbar, M.T., Rizwan, M., Jan, F., Wajidullah, Akhtar, N., Khattak, A. and Syed, S. 2021. Green Synthesis of Zinc Oxide (ZnO) Nanoparticles Using Aqueous Fruit Extracts of Myristicafragrans: Their Characterizations and Biological and Environmental Applications. ACS Omega, 6(14): 9709-9722. https://doi.org/10.1021/acsomega.1c00310

Gopinath, K., Gowri, S., Karthika, V. and Arumugam, A. 2014. Green synthesis of gold nanoparticles from fruit extract of Terminalia arjuna, for the enhanced seed germination activity of Gloriosa superba. Journal of Nanostructure in Chemistry, 4(3): 1-11.

https://doi.org/10.1007/s40097-014-0115-0

Gupta, M., Tomar, R.S., Kaushik, S., Mishra, R.K. and Sharma, D. 2018. Effective Antimicrobial Activity of Green ZnO Nano Particles of Catharanthus roseus. Frontiers in microbiology, 9. https://doi.org/10.3389/fmicb.2018.02030

Hemlata, Meena, P.R., Singh, A.P. and Tejavath, K.K. 2020. Biosynthesis of Silver Nanoparticles Using Cucumis prophetarum Aqueous Leaf Extract and Their Antibacterial and Antiproliferative Activity Against Cancer Cell Lines. ACS Omega, 5(10): 5520-5528.

https://doi.org/10.1021/acsomega.0c00155

Jain, S. and Mehata, M.S. 2017. Medicinal Plant Leaf Extract and Pure Flavonoid Mediated Green Synthesis of Silver Nanoparticles and their Enhanced Antibacterial Property. Scientific Reports, 7(1): 15867.

https://doi.org/10.1038/s41598-017-15724-8

Jobe, M.C., Mthiyane, D.M.N., Mwanza, M. and Onwudiwe, D.C. 2022. Biosynthesis of zinc oxide and silver/zinc oxide nanoparticles from Urgineaepigea for antibacterial and antioxidant applications. Heliyon, 8(12): e12243.

https://doi.org/10.1016/j.heliyon.2022.e12243

Khlebtsov, N., Trachuk, L.A. and Mel'nikov, A. 2005. The effect of the size, shape, and structure of metal nanoparticles on the dependence of their optical properties on the refractive index of a disperse medium. Optics and Spectroscopy, 98: 77-83. https://doi.org/10.1134/1.185804

Kilic, H.K., Cakmakci, T. and Sensoy, S. 2025. The application of nanoparticles on the physiological, morphological, enzyme activities, and nutrient uptake of lettuce under different irrigation regimes. Environment, Development and Sustainability. https://doi.org/10.1007/s10668-025-06120-8

Madanayake, N.H. and Adassooriya, N.M. 2021. Phytotoxicity of Nanomaterials in Agriculture. The Open Biotechnology Journal, 15: 109-118.

https://doi.org/10.2174/1874070702115010109

Malandrakis, A.A., Kavroulakis, N., Avramidou, M., Papadopoulou, K.K., Tsaniklidis, G. and Chrysikopoulos, C.V. 2021. Metal nanoparticles: Phytotoxicity on tomato and effect on symbiosis with the Fusarium solaniFsK strain. Science of The Total Environment, 787: 147606.

https://doi.org/10.1016/j.scitotenv.2021.147606

Maqsood, M.F., Shahbaz, M., Khalid, F., Rasheed, Y., Asif, K., Naz, N., Zulfiqar, U., Zulfiqar, F., Moosa, A., Alamer, K.H. and Attia, H. 2023. Biogenic nanoparticles application in agriculture for ROS mitigation and abiotic stress tolerance: A review. Plant Stress, 10: 100281.

https://doi.org/10.1016/j.stress.2023.100281

Mohamed, M.Y.A., Ferjani, H., Ogunjinmi, O.E., Jalouli, M. and Onwudiwe, D.C. 2024. Phyto-mediated synthesis of Ag, ZnO, and Ag/ZnO nanoparticles from leave extract of Solanum macrocarpon: Evaluation of their antioxidant and anticancer activities. InorganicaChimica Acta, 569: 122086.

https://doi.org/10.1016/j.ica.2024.122086

Muzammil, S., Ashraf, A. and Siddique, M.H. 2023. A review on toxicity of nanomaterials in agriculture: Current scenario and future prospects. 106(4): 368504231221672.

https://doi.org/10.1177/00368504231221672

Naseer, M., Aslam, U., Khalid, B. and Chen, B. 2020. Green route to synthesize Zinc Oxide Nanoparticles using leaf extracts of Cassia fistula and Melia azadarach and their antibacterial potential. Scientific Reports, 10(1): 9055.

https://doi.org/10.1038/s41598-020-65949-3

Osman, A.I., Zhang, Y., Farghali, M., Rashwan, A.K., Eltaweil, A.S., Abd El-Monaem, E.M., Mohamed, I.M.A., Badr, M.M., Ihara, I., Rooney, D.W. and Yap, P.-S. 2024. Synthesis of green nanoparticles for energy, biomedical, environmental, agricultural, and food applications: A review. Environmental Chemistry Letters, 22(2): 841-887.

https://doi.org/10.1007/s10311-023-01682-3

Rajiv, P., Rajeshwari, S. and Venckatesh, R. 2013. Bio-fabrication of zinc oxide nanoparticles using leaf extract of Parthenium hysterophorus L. and its size-dependent antifungal activity against plant fungal pathogens. Spectrochim Acta A Mol BiomolSpectrosc, 112: 384-387.

https://doi.org/10.1016/j.saa.2013.04.072

Rana, L., Kumar, M., Rajput, J., Kumar, N., Sow, S., Kumar, S., Kumar, A., Singh, S.N., Jha, C.K., Singh, A.K., Ranjan, S., Sahoo, R., Samanta, D., Nath, D., Panday, R. and Raigar, B.L. 2024. Nexus between nanotechnology and agricultural production systems: challenges and future prospects. Discover Applied Sciences, 6(11): 555.

https://doi.org/10.1039/D5EN00037H

Rutkowski, M., Krzemińska-Fiedorowicz, L., Khachatryan, K., Khachatryan, G., Kalisz, A. and Sękara, A. 2024. Impact of silver nanoparticles in alginate gels on seed germination, growth and stress biochemical parameters of cucumber seedlings. Plant Stress, 12: 100491.

https://doi.org/10.1016/j.stress.2024.100491

Saware, K. and Venkataraman, A. 2014. Biosynthesis and Characterization of Stable Silver Nanoparticles Using Ficusreligiosa Leaf Extract: A Mechanism Perspective. Journal of Cluster Science, 25(4): 1157-1171.

https://doi.org/10.1007/s10876-014-0697-1

Saxena, R., Kotnala, S., Bhatt, S.C., Uniyal, M., Rawat, B.S., Negi, P. and Riyal, M.K. 2025. A review on green synthesis of nanoparticles toward sustainable environment. Sustainable Chemistry for Climate Action, 6: 100071.

https://doi.org/10.1016/j.scca.2025.100071

Sembada, A.A. and Lenggoro, I.W. 2024. Transport of Nanoparticles into Plants and Their Detection Methods. 14(2).

https://doi.org/10.3390/nano14020131

Szőllősi, R., Molnár, Á., Kondak, S. and Kolbert, Z. 2020. Dual Effect of Nanomaterials on Germination and Seedling Growth: Stimulation vs. Phytotoxicity, Plants.

https://doi.org/10.3390/plants9121745

Talam, S., Karumuri, S.R. and Nagarjuna, G. 2012. Synthesis, Characterization, and Spectroscopic Properties of ZnO Nanoparticles. ISRN Nanotechnology, 2012.

https://doi.org/10.5402/2012/372505

Umavathi, S., Mahboob, S., Govindarajan, M., Al-Ghanim, K.A., Ahmed, Z., Virik, P., Al-Mulhm, N., Subash, M., Gopinath, K. and Kavitha, C. 2021. Green synthesis of ZnO nanoparticles for antimicrobial and vegetative growth applications: A novel approach for advancing efficient high quality health care to human wellbeing. Saudi J Biol Sci, 28(3): 1808-1815. https://doi.org/10.1016/j.sjbs.2020.12.025

Vishwanath, R. and Negi, B. 2021. Conventional and green methods of synthesis of silver nanoparticles and their antimicrobial properties. Current Research in Green and Sustainable Chemistry, 4: 100205.

https://doi.org/10.1016/j.crgsc.2021.100205

Wang, F.-H. and Chang, C.-L. 2016. Effect of substrate temperature on transparent conducting Al and F co-doped ZnO thin films prepared by rf magnetron sputtering. Applied Surface Science, 370. https://doi.org/10.1016/j.apsusc.2016.02.161

Zaman, W., Ayaz, A. and Park, S. 2025. Nanomaterials in Agriculture: A Pathway to Enhanced Plant Growth and Abiotic Stress Resistance, Plants. https://doi.org/10.3390/plants14050716

Zhang, D.H., Xue, Z.Y. and Wang, Q.P. 2002. The mechanisms of blue emission from ZnO films deposited on glass substrate by r.f. magnetron sputtering. Journal of Physics D: Applied Physics, 35(21): 2837.

https://doi.org/10.1088/0022-3727/35/21/321